

## Evaluation of Wavelets for Reduction of Motion Artifacts in Photoplethysmographic Signals

M. Raghuram<sup>1</sup>, K. Venu Madhav<sup>1</sup>, E. Hari Krishna<sup>2</sup>, and K. Ashoka Reddy<sup>3</sup>

<sup>1</sup> Dept. of E & I Engg, <sup>2</sup> Dept. of ECE, Kakatiya Institute of Technology & Science, Warangal, India.

<sup>3</sup> Dept. of ECE, KU College of Engineering & Technology, Kakatiya University, Warangal, India.

Email: ramcapri@yahoo.co.uk, kotturvenu@yahoo.com, hari\_etta@yahoo.co.in, reddy.ashok@yahoo.com

### ABSTRACT

*Photoplethysmographic (PPG) signals obtained at Red and Infrared wavelengths are utilized in pulse oximetry for estimation of arterial blood oxygen saturation (SpO<sub>2</sub>). Mostly inaccurate readings in a pulse oximeter arise when PPG signals are contaminated with motion artifacts (MA) due to the movement of patient and hence MA are a common cause of oximeter failure and loss of accuracy. This paper presents performance evaluation of different wavelets for the reduction of MA. Test results on the PPG signals recorded with frequently encountered artifacts (viz., horizontal, vertical and bending motions of finger) reveal that the estimated SpO<sub>2</sub> values from MA reduced PPGs using different wavelets are very close to each other. In addition, the Daubechies wavelet interestingly kept the respiratory information intact while effectively removing the MA from PPG signals. Hence, the work establishes that the Daubechies wavelet is the most preferred wavelet for pulse oximetry applications.*

Keywords: PPG, Motion artifact, Wavelet Transform.

### 1. INTRODUCTION

In Pulse Oximetry, two photoplethysmographic (PPG) signals are obtained by illuminating a part of the body of interest, at Red (R) and Infrared (IR) wavelengths, and acquiring either the reflected or transmitted light. The PPG signals are commonly contaminated with motion artifacts (MA) due to movement of the patient, resulting in inaccurate estimation of arterial oxygen saturation (SpO<sub>2</sub>) [1]. Hence, reduction of MA has been a challenging problem ever since the invention of pulse oximetry. There have been many attempts to reduce the influence of motion artifacts from corrupted PPG signals.

As the MA results in an in-band noise, adaptive filters [2]-[5] offer best solution compared to conventional moving average method [6]. Use of a synthetic reference signal estimated from the artifact-free part of the PPG signal [5] was also reported for reducing motion artifact. Significant improvements were observed by applying time-frequency methods like smoothed pseudo Wigner-Ville distribution [7], making use of the non-stationary nature of the PPG signals. It has also been demonstrated

that independent component analysis (ICA) can be applied to reduce the motion artifacts [8] by exploiting the independence between PPG and motion artifact signals. New processing methods meant for MA reduction, based on singular value decomposition (SVD) [9] and cycle-by-cycle Fourier series (CFSA) [10], extracted clean artifact free PPG signals preserving all the essential morphological features required, but are computationally intensive. Though Wavelet denoising approach has been examined in the past decades [11], no information has been published concerning comparative wavelet analysis for reduction of MA in PPG signals. In this paper, we evaluated wavelets for the reduction of MA from the PPG signal for reliable estimation of parameters like oxygen saturation and pulse rate. As the PPG contains the information concerned to heart rate, heart rate variability, blood pressure and respiration, an attempt is being made to identify the Wavelet which efficiently preserves the respiratory induced intensity variation while removing MA from the PPG.

### 2. MOTION ARTIFACT REDUCTION

The wavelet transform (WT) provides an alternative to the classical short-time Fourier transform (STFT), which uses a single analysis window. The WT uses short windows at high frequencies and long windows at low frequencies. Basically, the wavelets are classified into continuous wavelet transform (CWT) and discrete wavelet transform (DWT) [12].

The CWT is defined as the sum over all time of the signal multiplied by scaled, shifted versions of the wavelet function or alternatively as shown in the following equation:

$$CWT(a, \tau) = \frac{1}{\sqrt{a}} \int x(t) \psi\left(\frac{t-\tau}{a}\right) dt \quad (1)$$

where  $a$  is the scaling factor that stretches or compresses the function,  $\tau$  is the translation factor that shifts the mother wavelet along the axis,  $x(t)$  is an integral signal whose sum is to be multiplied by the translated mother wavelet denoted as  $\psi(t)$ , which is a function of the scaling and translation factors. The DWT is referred to as decomposition by wavelet filter banks, using two filters, a low pass filter (LPF) and a high pass filter (HPF) to decompose the signal into different scales shown in Fig 1.  $A_j$  is the approximated coefficients and  $D_j$  is the detailed co-efficients. The output coefficients of the LPF are called approximation coefficients, while the output

coefficients of the HPF are called detailed coefficients. The approximation signal may be passed down to be decomposed again by breaking the signal into many levels of lower resolution components and the decomposition process is iterative, called ‘multiple level decomposition’. Then the signal is reconstructed from the approximation and detailed coefficients as shown in Fig 2.

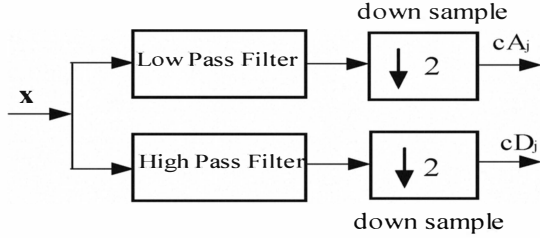


**Figure 1.** Wavelet Decomposition

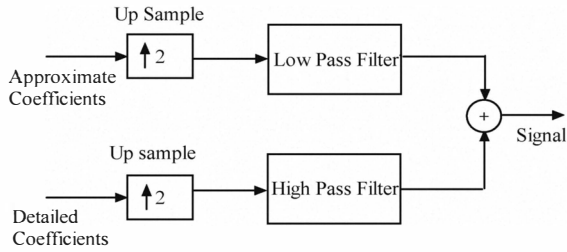


**Figure 2.** Wavelet Reconstruction

Only the last level of approximation is saved among all levels of detailed coefficients, which provides sufficient data to fully reconstruct the original signal using complementary filters.  $L$  is the length of the coefficients.

The wavelet transform is a convolution of the wavelet function  $\psi(t)$  with the signal  $x(t)$  and orthonormal dyadic discrete wavelets are associated with scaling functions  $\phi(t)$ . The scaling function can be convolved with the signal to produce approximation coefficients  $S$ . The discrete wavelet transform (DWT) can be given as

$$T_{m,n} = \int_{-\infty}^{\infty} x(t) \psi_{m,n}(t) dt \quad (2)$$

By choosing an orthonormal wavelet basis  $\psi_{m,n}(t)$  we can reconstruct the original. The approximation coefficient of the signal at the scale  $m$  and location  $n$  can be given as

$$S_{m,n} = \int_{-\infty}^{\infty} x(t) \phi_{m,n}(t) dt \quad (3)$$

The discrete input signal  $S_{0,N}$  is of finite length  $N$ , which is an integer power of 2:  $N = 2^M$ . Thus the range of scales that can be investigated is  $0 < m < M$ . A discrete approximation of the signal can be shown as

$$x_0(t) = x_M(t) + \sum_{m=1}^M d_m(t) \quad (4)$$

where the mean signal approximation at scale  $M$  is

$$x_M(t) = S_{M,n}(t) \phi_{M,n}(t) \quad (5)$$

and the detail signal approximation corresponding to scale  $m$  is defined for a finite length signal as

$$d_m(t) = \sum_{n=0}^{2^{M-m}-1} T_{m,n} \psi_{m,n}(t) \quad (6)$$

Adding the approximation of the signal at scale index  $M$  to the sum of all detail signal components across scales gives the approximation of the original signal at scale index 0. The signal approximation at a specific scale was a combination of the approximation and detail at the next lower scale.

$$x_m(t) = x_{m-1}(t) - d_m(t) \quad (7)$$

If scale  $m = 3$  was chosen, it can be shown that the signal approximation is given by

$$x_3(t) = x_0(t) - d_1(t) - d_2(t) - d_3(t) \quad (8)$$

In each step, there may be a successive stripping of high frequency information contained within the detailed signal,  $d_m(t)$ , which is an approximation of original signal. This is referred to as multi-resolution analysis of a signal using wavelet transform, and is the basis of our procedure.

The choice of the wavelet function depends on the type of application. The Haar wavelet function has the advantage of being simple to compute and easy to understand, whereas the Daubechies wavelet algorithm is conceptually more complex. But, it picks up detailed coefficients that were missed by the Haar. Selecting a wavelet function which closely matches the signal to be processed is of utmost importance in wavelet applications.

#### A. Motion Artifact Reduction using Wavelets

In wavelet processing, the test signals are transformed, thresholded and inverse-transformed. The general denoising procedure involves three steps [13], and the processing can be explained in clear way with the help of cascaded blocks shown below in Fig 3. Motion artifact (MA) reduced PPG signal can be obtained by processing the corrupted portion of the PPG signal as described in the steps below:

- 1) *Decomposition*: First choose any wavelet with proper selection of level  $N$ . Then, Compute the wavelet decomposition of the signal  $s$  at level  $N$ .
- 2) *Thresholding*: Appropriate threshold is applied to the detailed coefficients prior to the  $N^{\text{th}}$  level of decomposition
- 3) *Reconstruction*: Perform wavelet reconstruction using the original approximation coefficients of level  $N$  and the modified detailed coefficients of levels from 1 to  $N$ .

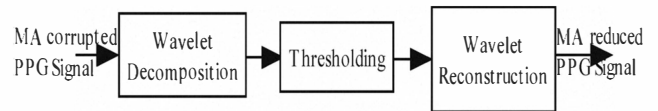


**Figure 3.** Wavelet Block processing for MA reduction

### 3. SIMULATION RESULTS

A prototype Photoplethysmograph was designed and developed with clip-on PPG sensor, housing a red LED and an IR LED on one side and a photodiode detector on the other side, and interfaced to the signal conditioning circuitry shown in Fig. 4. The red and IR PPG signals (samples of red and IR detector voltages) are acquired using an NI-DAQPad-6015 data acquisition system manufactured by National Instruments. To evaluate the performance of the wavelets, frequently encountered artifacts (horizontal, vertical and bending motions of finger) during post-operative recovery and intensive care were created intentionally during the PPG data recording process from subjects. These signals were sampled at 250Hz. A thorough literature review motivated us to consider the following wavelets for the task of motion artifact reduction: Daubechies, biorthogonal, reverse biorthogonal, symlet and Coiflet types of wavelets. The recorded PPG signal corrupted with motion artifact (for bending motion of finger) is depicted in Fig. 5. In order to test the efficacy, different wavelets were applied on the motion artifact corrupted PPG and the resulted MA reduced PPG signals along with their corresponding spectra are portrayed in Fig. 6, wherein the morphological features of the PPG were seen to be clearly restored. The Daubechies wavelet performs well in MA reduction restoring respiratory activity information involved in the low frequency region as shown in Fig. 6 (b2).

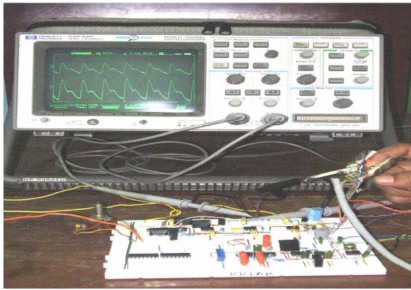


**Figure 4.** Developed prototype PPG analog front-end

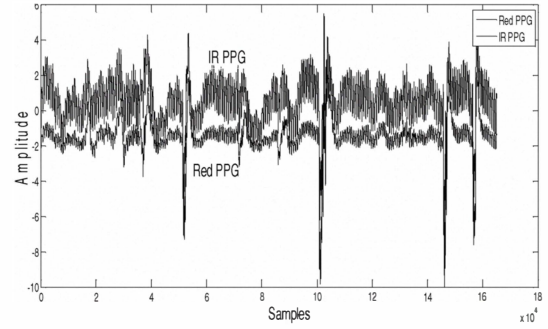


**Figure 5.** Artifact corrupted PPG data recorded from a volunteer

However, visual inspection of the filtered output did not reveal much information about the efficacy of wavelets. Hence, for performance evaluation,  $SpO_2$  values are estimated from MA reduced PPG signals.

#### A. $SpO_2$ Calculation

An artifact-free PPG signal is composed of clearly separable AC and DC parts. For the measurement of  $SpO_2$ , the DC parts of the red ( $DC_{Red}$ ) and Infrared ( $DC_{IR}$ ) PPG signals are extracted. Similarly the peak to peak values of the pulsatile components at the heart rate  $AC_{Red}$  and  $AC_{IR}$  of the red and IR PPG signals respectively are measured and the “ratio of ratios”  $R$  is estimated as [14]

$$R = \frac{(AC_{Red}/DC_{Red})}{(AC_{IR}/DC_{IR})} \quad (9)$$

Using  $R$  of (9),  $SpO_2$  is calculated using the relationship  $SpO_2 \% = (110 - 25R) \% \quad (10)$

Here, for performance comparison, the statistical analysis is made in terms of mean  $\pm$  Standard Deviation (SD) of  $R$  and then  $SpO_2$  values calculated using (10) from MA reduced PPG signals. It is observed from results of table I, that all the wavelets performed relatively well in estimating the  $SpO_2$  after reducing the MA by them.

In essence, the very fact is that most motion artifact reduction algorithms essentially disturb and sometimes remove the respiratory activity (0.2Hz-0.35 Hz), which is

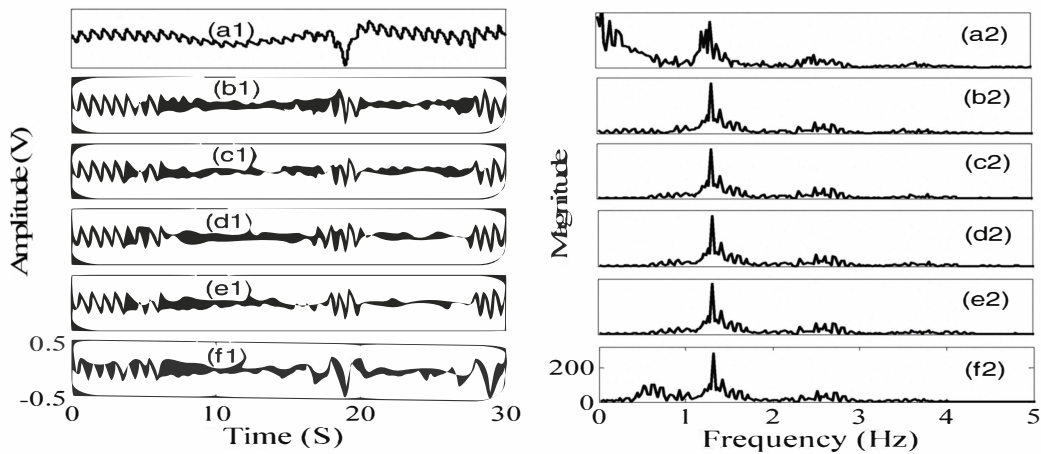


**Figure 6.** (a1) MA corrupted PPG, MA reduced PPG using (b1) Daubechies, (c1) biorthogonal (d1) reverse biorthogonal (e1) symlet (f1) Coiflet wavelets and their corresponding spectra of PPG from (b2) - (f2)

TABLE I. COMPUTED VALUES OF  $R$  AND  $SpO_2$  OF MA REDUCED PPG USING DIFFERENT WAVELETS

PPG recovered using wavelet	Horizontal motion		Vertical motion		Bending motion	
	$R$	$SpO_2$	$R$	$SpO_2$	$R$	$SpO_2$
db10	0.68±0.048	93%	0.720±0.059	92%	0.56±0.13	96%
bior 6.8	0.69±0.035	92.75%	0.730±0.052	91.75%	0.59±0.06	95.25%
rbio6.8	0.70±0.035	92.5%	0.724±0.055	91.90%	0.6±0.06	95%
sym8	0.70±0.036	92.5%	0.733±0.057	91.67%	0.604±0.067	94.9%
coif5	0.67±0.058	93.25%	0.729±0.060	91.75%	0.57±0.17	95.75%

close to the MA band of the PPG signal. The study presented here reveals an important observation, as seen from Fig. 6(b2), that the respiratory activity was not disturbed by the use of Daubechies Wavelets in attempting to reduce the MA.

#### 4. CONCLUSION

The PPG signals are invariably corrupted by artifacts whenever the patient connected to the pulse oximeter moves. Hence, the reliability of pulse oximeters in estimating the  $SpO_2$  is affected by motion artifacts (MA) introduced in to the PPG signals. This paper presented the performance evaluation of different wavelets for reduction of MA from PPG signals. Wavelet analysis has been carried out on the PPGs corrupted with frequently encountered motion artifacts such as bending finger, vertical and horizontal motions with a view to reduce the MA and resorting respiratory activity in PPG signals. Experimental results revealed two important facts. Firstly, the  $SpO_2$  values estimated from MA reduced PPG signals by different wavelets are relatively near to each other and finally the Daubechies wavelet exhibited superior performance over others in resorting respiratory information while removing MA. Hence, Daubechies wavelet is the most preferred one for pulse oximetry applications.

#### REFERENCES

- [1] J. G. Webster, Design of Pulse Oximeters, *Taylor & Francis Group*, NY, 1997.
- [2] B. Barreto, L. M. Vicente and I. K. Persad, "Adaptive cancellation of motion artifact in photoplethysmographic blood volume pulse measurements for exercise evaluation," in *Proc. IEEE-EMBC and CMBC*, vol. 2, pp. 983-984, 20-23 sept., 1995.
- [3] R. Relente and L. G. Sison, "Characterization and adaptive filtering of motion artifacts in pulse oximetry using accelerometers", in *Proc. Conf. EMGS/BMES, Houston, TX, USA*, pp. 1769-1770, 23-26 Oct., 2002.
- [4] K. W. Chan and Y. T. Zhang, "Adaptive reduction of motion artifact from photoplethysmographic recordings using a variable step-size LMS filter," in *Proc. IEEE Sensors*, vol. 2, pp. 1343- 1346, 2002.
- [5] F. M. Coetzee and Z. Elghazzawi, "Noise-resistant pulse oximetry using a synthetic reference signal," *IEEE trans. Biomed. Engg.*, vol. 47, no. 8, pp. 1018-1026, 2000.
- [6] T. L. Rusch, R. Sankar and J. E. Scharf, "Signal processing methods for pulse oximetry," *Comput. Biol. Med.*, vol. 26, no. 2, pp. 143- 159, 1996.
- [7] Y. S. Yan, C. C. Poon and Y. T. Zhang, "Reduction of motion artifact in pulse oximetry by smoothed pseudo Wigner-Ville distribution," *J Neuroengineering. Rehabil.*, 2005, 2-3, available from <http://www.jneuroengrehab.com/content/2/1/3>.
- [8] S. Kim and S. K. Yoo, "Motion artifact reduction in photoplethysmography using independent component analysis," *IEEE Trans. Biomed. Eng.*, vol. 53, No. 3, pp. 566- 568, 2006.
- [9] K. A. Reddy and V. J. Kumar, "Motion artifact reduction in photoplethysmographic signals using singular value decomposition," in *24<sup>th</sup> Int. Conf. IEEE, IMTC-2007*, pp. 1-5, Warsaw, Poland, 1-3 May, 2007.
- [10] K. A. Reddy, B. George and V. J. Kumar, "Use of Fourier analysis for motion artifact reduction and data compression of Photoplethysmographic signals", *IEEE Trans. Instrum. Meas.*, vol. 58, no.5, pp. 1706-1711, 2009.
- [11] M. Lee and Y. T. Zhang, "Reduction of motion artifacts from photoplethysmographic recordings using a wavelet denoising approach," in *Proc. IEEE EMBS Asian-Pacific Conf. on Biomed. Engg.*, pp. 194- 195, 20-22 Oct., 2003.
- [12] S. Hans-Gorge, "Wavelets and signal processing; an application-based introduction," Newyork: Springer, 2005.
- [13] M. Alfaouri and K. Daqrouq, "ECG signal denoising by wavelet transform thresholding," *American Journal of Applied Sciences*, vol. 5, no. 3, pp. 276-281, 2008.
- [14] K. A. Reddy, B. George, N. M. Mohan and V. J. Kumar, "A Novel Calibration-Free Method for Measurement of Oxygen Saturation in Arterial Blood", *IEEE Trans on Instrum. Meas.*, vol. 58, no. 5, pp 1699-1705, May 2009.